Available online at www.sciencedirect.com
SCIENCE DIRECT®
Journal of Solid State Chemistry 178 (2005) 429–434
JOURNAL OF SOLID STATE CHEMISTRY
www.elsevier.com/locate/jssc

Can magnetic circular dichroism tackle the problem of site symmetry in solutions?

Linda Fluyt*, Kris Driesen, Christiane Görller-Walrand

Department of Chemistry, Katholieke Universiteit Leuven, Celestijnenlaan 200F, B-3001 Leuven, Belgium

Received 27 April 2004; received in revised form 15 July 2004; accepted 28 July 2004
Available online 18 September 2004

Abstract

A new approach to unravel the site symmetry of lanthanides in solutions is presented. The magnetic circular dichroism spectra of Eu^{3+} in the symmetries D_{3h}, C_{4v} and D_{2d} are simulated. In these simulations, the main idea is to introduce the magnetic field along a 3-fold axis, being the resultant of the three equivalent *X*-, *Y*- and *Z*-direction of a cube. This implies that the parallel and perpendicular Zeeman effects are taken into account simultaneously.

Keywords: Lanthanides; Magnetic circular dichroism; Spectroscopy; Solutions; Site symmetry

1. Introduction

For many applications, it is a challenging problem to provide significant information concerning the geometry and coordination number of lanthanide complexes in solution.

Especially the applications of rare earths in biochemistry have attracted widespread attention, because the luminescent properties of lanthanides can be used to probe metal ion bonding sites in biological macromolecules. This article aims to propose our view on magnetic circular dichroism (MCD) spectra in order to tackle the problem of site symmetry in solutions or amorphous media.

The relationship between the site symmetry and the experimental MCD spectra is investigated by simulations of the MCD transitions. These simulations involve the calculation of the Zeeman energy levels and the transition intensities according to the additive ligand field parameter model.

The backbone of the computer programs used for these calculations can be found in the original well-known crystal field programs from the group of Carnall [1] which afterwards have been rewritten and extended by Reid [2].

The main idea established here is that simulations for MCD transitions in media with randomly oriented molecules can be performed by applying the magnetic field along a trigonal axis, being the resultant of the three equivalent directions in a cube (see Fig. 1).

2. Theoretical background

The MCD technique is based on the Zeeman effect induced in every molecule that is placed in a longitudinal magnetic field with respect to the propagation direction of the light.

According to the commonly used Stephens mechanism, the MCD curves are described in terms of *A*-, *B*- and *C*-term [3]. In spite of the beauty of this description, it soon became clear to most authors that the assumptions made in this model are not likely to be adequate for the majority of lanthanide spectra. We will show in our conclusion that these terms are even very misleading in interpreting the spectra of lanthanide ions in solutions. This is essentially due to the small bandwidth

*Corresponding author. Fax: +32-16-32-79-92.
E-mail address: Linda.Fluyt@chem.kuleuven.ac.be (L. Fluyt).

0022-4596/$ - see front matter © 2004 Elsevier Inc. All rights reserved.
doi:10.1016/j.jssc.2004.07.047

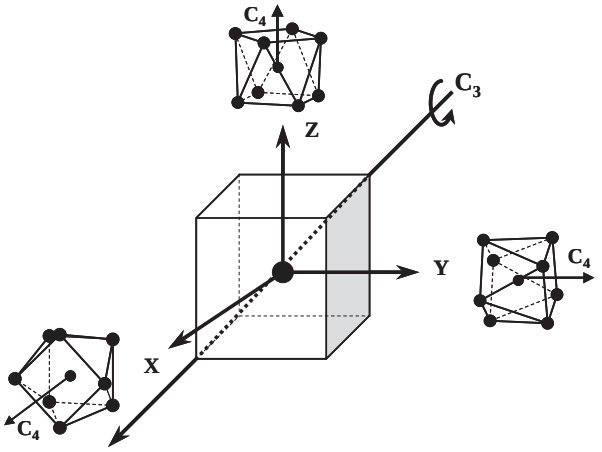

Fig. 1. Three C_{4v} orientations (respresentative for KY_3F_{10}/Eu^{3+}) toward the *X*-, *Y*- and *Z*-direction and the resultant 3-fold axis of a cube.

of the peaks and to the weakness of the crystal field effect with respect to that of the Zeeman effect. It is therefore more advisable to go back to the essence of Zeeman spectroscopy and interpret the transitions in MCD spectra of lanthanide ions as Zeeman transitions that are governed by selection rules for circularly polarized light. By convention, absorption of left circularly polarized light gives a positive signal.

The case of random orientation of molecules in solutions can be regarded as one-third of the sites having their main axis along *X*, one-third along *Y*, and one-third along *Z*. This situation shows a very interesting resemblance with the KY_3F_{10}/Eu^{3+} crystal [4]. Indeed this uniaxial cubic crystal allows MCD measurements with light propagating along the optical axis. In this crystal, one-third of the sites have their main axis along the crystallographic *Z*-axis; one-third have them along the *X*-axis and another third along the *Y*-axis (see Fig. 1). For one-third of the sites, the parallel Zeeman effect is induced because the crystal *Z*-axis corresponds to the main axis (*z*) of the site while for two-third of the sites the perpendicular Zeeman effect is induced as the crystallographic main axis corresponds to the *x*- and *y*-site axes. The final MCD spectrum is a superposition of $\mathbf{H_z}$, $\mathbf{H_x}$ and $\mathbf{H_y}$.

So this KY_3F_{10}/Eu^{3+} crystal provides a rather unique tool for experimental verification of the parallel and perpendicular Zeeman effect.

Attention will be focused on the pure magnetic dipole $^5D_1 \leftarrow ^7F_0$ transition and the induced electric dipole $^5D_2 \leftarrow ^7F_0$ of the Eu^{3+} ion.

2.1. The $^5D_1 \leftarrow ^7F_0$ transition of Eu^{3+} in an axial symmetry with main axis $n>2$

In an axial symmetry (e.g., C_{4v}) $J=1$ splits in a $M_J = \pm 1$ state and a $M_J = 0$ state. A longitudinal magnetic field yields a linear Zeeman splitting for $M_J = \pm 1$ and a field independent behavior for $M_J = 0$, corresponding to the parallel Zeeman effect described by the Hamiltonian $\mathbf{H_z}$. According to the selection rules for magnetic dipole transitions [5,6] the $^5D_1 \leftarrow ^7F_0$ will always look like what is called a positive *A*-term in the Stephens formalism. We then consider the effect of a perpendicular magnetic field corresponding to the operators $\mathbf{H_x}$ and $\mathbf{H_y}$. The operators will mix in $|\pm 1>$ and $|0>$ as a second-order effect and a non-linearity in the Zeeman pattern is obtained. For convenience, we will further use $\mathbf{H_x}$ which effect can also be described by a cyclic perturbation of the axis $x \rightarrow y \rightarrow z \rightarrow x$. The same considerations are true for $\mathbf{H_y}$ (with an $x \leftarrow y \leftarrow z \leftarrow x$ transformation). The magnetic fields applied in the experiments have a strength of 1 T for the electromagnet and a strength of 7 T for the superconducting magnet. This corresponds respectively to a Zeeman splitting of ± 1 and $\pm 5\,cm^{-1}$. For the small magnetic field of 1 T, the perpendicular Zeeman effect only slightly affects the energy, but do affect the wave functions largely.

In Fig. 2, it is illustrated how one component of the degenerate state mixes in with $|0>$ in the original coordinate system. The result is that the upper function achieves $|+1>$ character while the lower function achieves $|-1>$ character so that left circularly polarized light is absorbed at high energy leading to a positive signal. An equivalent negative signal is predicted at the energy corresponding to the *z* polarized absorption in the original crystal field scheme (left energy-level scheme in Fig. 2).

2.2. The $^5D_2 \leftarrow ^7F_0$-induced electric dipole transition of Eu^{3+}

For this type of transition mechanism, it is opportune to keep in mind the physical meaning of the Judd–Ofelt parameters $A_{\lambda tp}$ (later more commonly symbolized in the literature by $B_{\lambda kq}$). The nice idea expressed by Judd in his famous paper [7] is that the intensity of lanthanide spectra is induced through the admixture in the *f* configuration of opposite parity configurations (*d* or *g*). This occurs by the odd crystal field potential term described by spherical tensor operators C_q^k (with *k* odd). In this so-called static crystal field model, the intensity is governed by the selection rule [5]:

$$M_{J'} - M_J = -(q+\rho),$$

where M_J is the ground state, $M_{J'}$ the excited state, *q* the odd crystal field component, ρ the polarization of the light $(0, +1, -1)$.

This selection rule can be reinterpreted for MCD as follows. The static dipole intensity corresponding to absorption of left circularly polarized light, and thus giving a positive signal, is always described by a *q* component that mixes in an odd parity state with

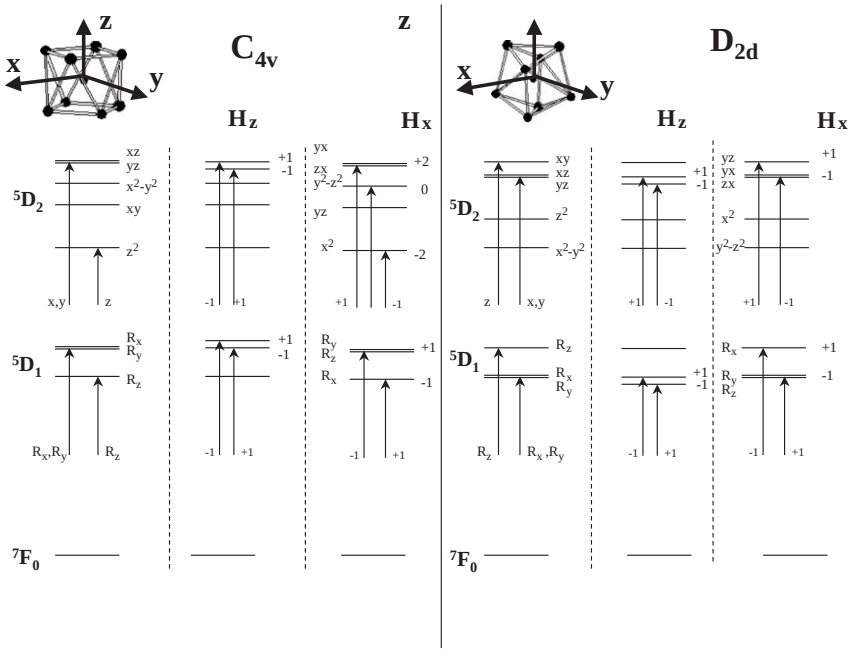

Fig. 2. Energy levels and MCD-transitions ($\mathbf{H_z}$ for the parallel and $\mathbf{H_x}$ and $\mathbf{H_y}$ for the perpendicular Zeeman effect) for the $^5D_{2,1} \leftarrow ^7F_0$ transitions for Eu^{3+} in C_{4v}- and D_{2d}-symmetry.

$M_J = +1$. The admixture of $M_J = -1$ leads obviously to the negative sign in the used MCD convention.

For the $^5D_2 \leftarrow ^7F_0$ transition, if we assume in a first approximation no J mixing, the odd crystal field terms will have $k = 1$ and $k = 3$.

2.3. The $^5D_2 \leftarrow ^7F_0$ transition of Eu^{3+} in C_{4v}, D_{2d} and D_{3h} symmetries

In this section, we consider the $^5D_2 \leftarrow ^7F_0$ transition for three symmetries: C_{4v} (slight distortion of D_{4d}), D_{2d} and D_{3h}, that characterize the coordination polyhedron of many lanthanide complexes namely the square antiprism (SAP), the dodecahedron (Dod) and the tricapped trigonal prism (TCTP). In view of keeping our model as simple as possible the angular polar coordinates [15] of the ligands (θ and φ) are those of the ideal symmetries, although they are close to the crystallographic data. For the SAP, we consider the case of KY_3F_{10}/Eu^{3+} where the site symmetry is C_{4v} due to a small distortion on D_{4d} ($\theta = \theta_{\text{cubic}}$). For the Dod we use the $LiYF_4/Eu^{3+}$ complex where θ_A and θ_B differ from the cubic angle by $\pm 15^\circ$. For the TCTP, we chose the europiumoxydiacetate. A value of $\theta = 45^\circ$ and $\theta = \pi - 45^\circ$ for the six ligands out of the equatorial plane implies a B_0^2-parameter that is equal to zero. In the simulations, a small B_0^2-parameter has been used so that a splitting of the $^5D_1$ level is observed. As already mentioned J mixing is not considered here because it will not affect the qualitative conclusions of this paper.

In Figs. 2 and 3, *the parallel Zeeman splitting* pattern and the absorption of circular polarized light is given under the heading $\mathbf{H_z}$.

The energy diagrams are labeled according to the base functions that in fact describe the real set of d-orbitals.

In Table 1, the odd crystal field terms for these three symmetries are given in the second column. Taking into account the static crystal field, the intensity occurs through the matrix elements that are given in the third column.

In these matrix elements, the ket function contains the M_J-quantum number of the $d(g)$-configuration that mixes in with the f-configuration (bra function) under the odd crystal field. Looking at the set of d-orbitals it is found that $|+1\rangle$, respectively, mixes with $\langle +1|$ for C_{4v}, with $\langle -1|$ for D_{2d} and with $\langle -2|$ for D_{3h}. As left circularly polarized light is absorbed to the $|+1\rangle$ level, the result is absorption of left circularly polarized light to the upper component in the case of C_{4v}, while absorption occurs to the lower component in D_{2d} and D_{3h}.

This is indeed confirmed experimentally for KY_3F_{10}/Eu^{3+} (C_{4v}) [9,10] and $LiYF_4/Eu^{3+}$ (D_{2d}) [11]. For D_{3h}, the predicted negative signs are demonstrated in single crystals with a distorted D_{3h}-symmetry, e.g., europiumoxydiacetate (D_3) [12] and other symmetries not considered here like LaF_3/Eu^{3+} (C_{2v}) [13] and $EuCl_6^{3-}$(D_2) [14]. So far for the classic parallel Zeeman effect.

Now the development of *the perpendicular Zeeman effect* is made clear.

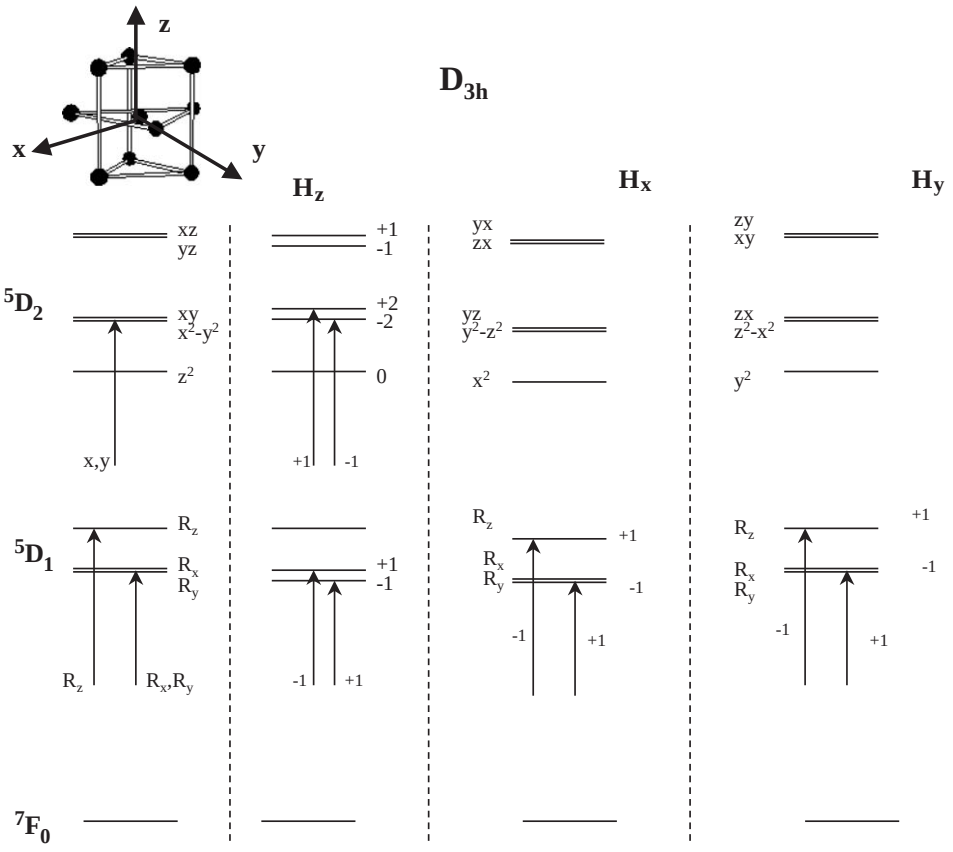

Fig. 3. Energy levels and MCD-transitions ($\mathbf{H_z}$ for the parallel and $\mathbf{H_x}$, $\mathbf{H_y}$ for the perpendicular Zeeman effect) for the ${}^5D_{2,1} \leftarrow {}^7F_0$ transitions for Eu^{3+} in D_{3h}-symmetry.

Table 1
Relevant tesseral harmonics for intensity calculations before and after rotations $x \to y \to z \to x$ and $x \leftarrow y \leftarrow z \leftarrow x$ [8]

Symmetry	Odd CF[a] $\mathbf{H_z}$	Intensity matrix elements[b]	Odd CF $x \to y \to z \to x$	Odd CF $x \leftarrow y \leftarrow z \leftarrow x$
C_{4v}	$\mathbf{C}_0^1$ $\mathbf{C}_0^3$	$\langle \pm 1 \vert C_0^1 + C_0^3 \vert \pm 1 \rangle$	$\mathbf{C}_1^1$ $-\frac{\sqrt{6}}{4}\mathbf{C}_1^3 + \frac{\sqrt{10}}{4}\mathbf{C}_3^3$	$\mathbf{S}_1^1$ $-\frac{\sqrt{6}}{4}\mathbf{S}_1^3 - \frac{\sqrt{10}}{4}\mathbf{S}_3^3$
D_{2d}	$\mathbf{S}_2^3 = \frac{i}{\sqrt{2}}(C_{-2}^3 - C_2^3)$	$\langle \mp 1 \vert C_{\mp 2}^3 \vert \pm 1 \rangle$	$\mathbf{S}_2^3$	$\mathbf{S}_2^3$
D_{3h}	$\mathbf{S}_3^3 = \frac{i}{\sqrt{2}}(C_{-3}^3 + C_3^3)$	$\langle \mp 2 \vert C_{\mp 3}^3 \vert \pm 1 \rangle$	$-\frac{\sqrt{10}}{4}\mathbf{C}_0^3 - \frac{\sqrt{6}}{4}\mathbf{C}_2^3$	$\frac{\sqrt{15}}{4}\mathbf{C}_1^3 - \frac{1}{4}\mathbf{C}_3^3$

[a]With $\mathbf{S}_q^k$ and $\mathbf{C}_q^k$ tesseral and C_q^k spherical harmonics.
[b]Odd crystal field terms acting between the wavefunction (M_J-quantum number) of the f-configuration in the bra and the wavefunction of the mixing configuration in the ket.

The energy diagram is considered in the rotation schemes $x \to y \to z \to x$ and $x \leftarrow y \leftarrow z \leftarrow x$ [8]. Now absorption of circularly polarized light is governed by the rotated odd crystal field terms. The relevant odd crystal field terms are given in Table 1.

For D_{2d} it is very straightforward to verify that the intensity for absorption of circularly polarized light at the higher energy occurs through the matrix element $\langle +1 \vert C_{+2}^3 \vert -1 \rangle$, so that a negative MCD signal is found at this energy.

For C_{4v} the same conclusion can be obtained although a combination of spherical harmonics after rotation makes the prediction of the polarization of the absorbed light more elaborate.

The signal of opposite sign is predicted at lower energy corresponding to the z polarized absorption in C_{4v} and to the x, y polarized absorption in D_{2d}. For D_{3h} the interplay of matrix elements compensates so that no intensity is induced which differentiates absorption from left and right circularly polarized light.

2.4. The magnetic field along the trigonal axis

This point is indeed inspired by the case of a cubic crystal like KY_3F_{10}/Eu^{3+} [9] where $\mathbf{H_z}$, $\mathbf{H_x}$ and $\mathbf{H_y}$ can be measured simultaneously on three sites with main axis following X, Y, Z. The idea is to simulate what would be the effect of applying the magnetic field along the trigonal axis and propagating the light along this axis. The three sites become now equivalent with respect to the field and the light. Moreover, a unique energy diagram is obtained corresponding to the application of the Zeeman operator:

$$\frac{1}{\sqrt{3}}\mathbf{H_z}+\frac{1}{\sqrt{3}}\mathbf{H_x}+\frac{1}{\sqrt{3}}\mathbf{H_y}.$$

The simulation of the MCD signals is given in Fig. 4.

Focusing on the $^5D_2 \leftarrow {}^7F_0$ transition it is clear that for the C_{4v} symmetry a positive signal appears at high energy followed after a very short energy gap by a negative signal that is larger in magnitude. The difference in magnitude corresponds to the positive signal at lower energy. This means that left circularly polarized light is absorbed to the higher Zeeman component, labeled $+1$ after applying $\mathbf{H_z}$. Right circularly polarized light is absorbed to the lower component -1 due to $\mathbf{H_z}$ and to the Zeeman component that originates from the yx crystal field level that after applying $\mathbf{H_x}$ and $\mathbf{H_y}$, mainly consists out of $+2$ character. The signal at lower energy is due to the z polarized absorption (z^2 becoming x^2).

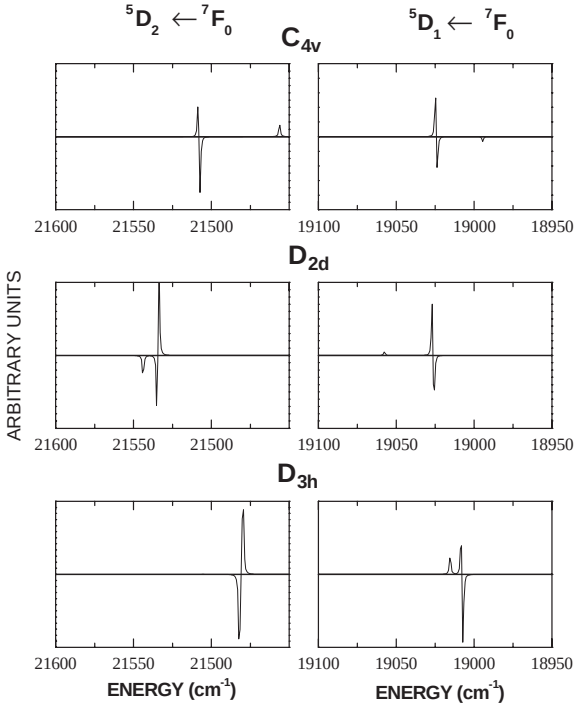

Fig. 4. Simulated MCD-spectra for $^5D_{2,1} \leftarrow {}^7F_0$ transitions for Eu^{3+} in C_{4v}, D_{2d} and D_{3h}-symmetry.

Analogous simulations are performed for D_{2d} and D_{3h}.

3. Conclusions

Finally, the model can be expanded to randomly oriented systems like solutions. As already mentioned, the relationship with the cubic structure is clear. In order to reproduce the spectra of lanthanide ions in solutions only the bandwidth has to be enlarged and the model simulations reveal that for the $^5D_2 \leftarrow {}^7F_0$ transition the different single crystal site symmetries lead to different signals.

In the case of the SAP, the signal is spread over the whole spectral region with eventually at higher energy a positive signal. If the bandshape is very large, this positive contribution disappears under the negative part.

For the Dod, we will never observe a positive signal at the high-energy side. Moreover, the signals are packed within a relatively small energy region. This is related to the small-energy gap between the xy and the degenerate xz, yz levels. As a Dod can be considered as a distortion of a cube (degenerate xy, xz and yz levels) this splitting and thereby the spread of the observed MCD signals reflects the distortion towards the ideal symmetry [15].

The TCTP clearly generates a signal with the shape of the derivative of an absorption band in the middle of the spectral region; with no additional possibility of other signals.

In the MCD signal in solutions, the contribution of the perpendicular Zeeman effect is important, meaning that the z polarized absorption plays a very important role.

Going back to the classical MCD formalism the clue point is that the transitions to the $^5D_2$ state will in most cases appear as a negative pseudo A-term. This is very misleading in drawing conclusions because the positive signals are often hidden by the negative signals.

The weak point in the MCD technique used so far is just what makes it so attracting in the Stephens formalism: the alternating measurement of left and right circularly polarized light absorption.

As soon as in a small wavelength region absorption of one type of polarization is dominant, the final signal has only one sign. This was indeed the same conclusion for the C-term where due to a population effect with a temperature change, in most situations only a positive or negative signal is obtained.

We can thus conclude that for solutions, Zeeman spectroscopy should be done with a light beam of fixed circularly polarization so that the complete signal can be recorded. Even for broad bands, the sign properties of the signal will then unambiguously lead to definite conclusions.

Acknowledgments

We thank M.F. Reid from the University of Canterbury (New Zealand) for the use of his computer programs. We thank FWO-Flanders (Project G.0117.03) and the GOA (Project 03/03) for the financial support. Kris Driesen is also indebted to the FWO-Flanders

References

[1] W.T. Carnall, H. Crosswhite, Crystal Field Programs for 4f-Configurations, Argonne National Laboratory, Argonne, IL, 1977.
[2] M.F. Reid, F-Shell Empirical Programs, University of Canterbury, New Zealand, 1988.
[3] P.J. Stephens, J. Chem. Phys. 52 (1970) 3489–3516.
[4] J.W. Pierce, H.Y.P. Hong, Proceedings of the Tenth Rare Earth Research Conference, Carefree, 1974, p. 527.
[5] C. Görller-Walrand, K. Binnemans, in: K.A. Gschneidner Jr., L. Eyring (Eds.), Handbook on the Physics and Chemistry of Rare Earths, Vol. 25, North-Holland, Amsterdam, 1998, p. 146 (Chapter 167).
[6] C. Görller-Walrand, K. Binnemans, Bull. Soc. Chim. Belg. 106 (1997) 685–689.
[7] B.R. Judd, Phys. Rev. 127 (1962) 750–761.
[8] J.L. Prather, Atomic Energy Levels in Crystals, NBS, Washington, 1961.
[9] L. Fluyt, K. Heyde, C. Görller-Walrand, Rare Earths '98 Materials Science Forum, Vol. 315–3, 1999, pp. 424–430.
[10] C. Görller-Walrand, M. Behets, P. Porcher, I. Laursen, J. Chem. Phys. 83–9 (1985) 4329–4337.
[11] L. Fluyt, K. Binnemans, C. Görller-Walrand, J. Alloys Compd. 225 (1995) 71–74.
[12] C. Görller-Walrand, P. Verhoeven, J. D'Olieslager, L. Fluyt, K. Binnemans, J. Chem. Phys. 100–2 (1994) 815–823.
[13] I. Couwenberg, C. Görller-Walrand, J. Alloys Compd. 275–277 (1998) 388–392.
[14] C. Görller-Walrand, N. De Moitié-Neyt, Y. Beyens, J.C. Bünzli, J. Chem. Phys. 77–5 (1982) 2261–2265.
[15] C. Görller-Walrand, K. Binnemans, in: K.A. Gschneidner Jr., L. Eyring (Eds.), Handbook on the Physics and Chemistry of Rare Earths, Vol. 23, North-Holland, Amsterdam, 1996, p. 213 (Chapter 155).